29 May 2010, 8:00 am - 9:30 am

Experimental Investigation of Plastic Demands on Piles During Lateral Spread-Induced Loads

Barbara J. Chang
University of California San Diego, La Jolla, CA

Tara C. Hutchinson
University of California San Diego, La Jolla, CA

Fifth International Conference on
Recent Advances in Geotechnical Earthquake Engineering and Soil Dynamics
and Symposium in Honor of Professor I.M. Idriss
May 24-29, 2010 • San Diego, California

EXPERIMENTAL INVESTIGATION OF PLASTIC DEMANDS ON PILES DURING LATERAL SPREAD-INDUCED LOADS

Barbara J. Chang
University of California, San Diego
La Jolla, California-USA 92122

Tara C. Hutchinson
University of California, San Diego
La Jolla, California-USA 92122

ABSTRACT

Past earthquakes have demonstrated that lateral spreading from liquefaction of the soil may cause undesirable movement and potential failure to the below ground portion of a pile foundation. For a multi-layer soil profile, the case of a dense crust layer overlying a liquefiable soil layer may create large localized plastic demands in the piles. To study this behavior and provide detailed data for use in model validation studies, a one-g shaking table experiment was conducted considering a single reinforced concrete pile embedded in a 3-layer soil system. The model pile of 10 inch diameter was tested in a sloped laminar soil box (70 in x 154 in x 74 in) to study its response to seismic kinematic loading. Inertial load effects were isolated from kinematic effects by designing the specimen without an inertial mass at the top. The test specimen was designed at the lower bound of typical design (low strength and stiffness) to promote yielding. The pile was extended 4D (where D = pile diameter) above the ground surface and penetrated 7D into a stiff uppermost crust (2.5D thick) overlying a middle saturated loose sand layer (2.5D thick) and a lower dense layer of sand (2.0D thick). The specimen was subjected to increasing amplitude ground motions to induce liquefaction and lateral spreading loads. Results indicate significant plastic demands localized at the crust-liquefiable layer interface.

INTRODUCTION

Lateral spreading from liquefaction of the soil may cause undesirable movement and potential failure to the below ground portion of a pile foundation. Many case histories describe severe to minor damage of structures and piles embedded in soils susceptible to liquefaction and/or lateral spreading-induced loads. (Yasuda and Berrill, 2000)

For example, the 1995 Hyogoken-Nambu earthquake was responsible for the damage of numerous substructures in reclaimed land along the coastline of Kobe (Tokimatsu and Asaka, 1998). In this region of Kobe, the deep foundations that are used generally consist of piles, which are precast concrete, steel pipe, or cast-in-place concrete. In areas where lateral spreading was caused by liquefaction, the pattern of damage found on the piles indicate that in addition to inertial forces from the superstructure, kinematic forces from the dynamic and permanent ground displacement contributed to pile damage. Tokimatsu and Asaka describe a building near the waterfront with piles that were deformed from lateral spreading caused by the earthquake. The contribution from kinematic forces are indicated by the deformed shape of the piles with damage from horizontal cracks at the bottom of liquefiable layer of soil, close to the interface between the liquefied layer and the non-liquefied layer below. This region of cracking indicates local plastic demands on the pile. During liquefaction, large differences in stiffness between these layers are present.

Typical structures generally have a significant superstructure mass supported by a deep foundation. A pile with a superstructure attached is affected more by inertial forces from the superstructure mass than the kinematic forces from the soil. A pile with no mass (attached to the top) is affected solely by the kinematic forces from the soil. Contrary to earlier thinking, liquefaction of the soil causes an increase in the shear force (in the pile) due to kinematic effects (more so than shear forces caused by the mass superstructure) (Tokimatsu *et al.* 2005). For this reason, experiments have been conducted on single piles or pile groups without attached superstructure masses to exclusively study the kinematic effects from the soil on pile stresses.

A study by Martin and Chen (2004) discuss the response of piles from lateral spreading based on two case histories.

Vertical and inertial loads from the superstructure were ignored, and only the permanent ground displacement was considered as the lateral loading mechanism. Results of FLAC3D finite difference analyses provide favorable comparison with the case histories, supporting the use of the modeling approach to account for lateral spreading. Investigation of soil and pile parameters showed that the relative stiffness between the pile and soil are important in predicting the failure modes of the pile and the soil. When the stiffness of the pile is high with respect to the soil, forces acting on the pile do not increase, which implies that the soil flows around the pile. A softer pile with respect the soil causes a lowering of lateral load acting on the pile; this implies deflection of the pile caused by the soil. With multiple soil layers of widely differing stiffness, a pile which is embedded through a saturated soil layer may have differing response (during an earthquake) dependant on the surrounding soil stratum.

Centrifuge experiments of piles and liquefying soil layers by Wilson et. al. (2000) have studied the soil-pile interaction in detail. Single pile and group pile supported structures were tested in multiple layers of saturated soil consisting of a loose or medium sand overlying a dense sand. Tests examined the soil-pile interaction which was able to be directly quantified from the back calculated p-y behavior of a well instrumented single pile-supported structure. Wilson et. al. concludes that the lateral p-y resistance of liquefied sand is significantly affected by relation density, cyclic degradation, excess pore pressures, phase transformation behavior, prior displacement history, and loading rate of the entire system.

Brandenberg et. al [2005] tested eight pile models on the UC Davis centrifuge to study the behavior of single piles and pile groups in liquefiable and laterally spreading ground. Pile diameters ranged from 0.36 meters to 1.45 meters for single piles and 0.73 to 1.17 meters for pile groups. The soil profile was a sloping gradient of a non-liquefied crust over liquefiable loose sand over dense sand. Realistic earthquake ground motions with peak base acceleration of 0.13g to 1.00 g were used as the base input. Conclusions from the tests show that the direction of the lateral loads from the varying soil layers depends on the direction of the incremental and total relative displacement of the pile and the soil. These in turn are dependent on the relative pile to soil stiffness, the deformation of the soil layers, and the load applied by the nonliquefied crust.

Pile response to kinematic effects has also been studied at the centrifuge at Rensselaer Polytechnic Institute [(Abdoun and Dobry, 2002) (Abdoun et. al. 2003) and (Dobry et. al. 2003)]. Eight centrifuge models of single and group piles in an inclined laminar soil box with multilayer soils were subjected to earthquake ground motions. Liquefaction and lateral spreading of the loose Nevada sand layer (Dr = 40%) was observed for the models. In all cases, the bending moment of the pile(s) was largest at the boundary between the liquefied and nonliquefied soil layers.

Centrifuge modeling has studied this problem caused by differential stiffness of the soil layers. This paper discusses experimental results on this specific phenomenon of differential stiffness for a 1-g shaking table test of a reinforced-concrete pile embedded in a multilayer soil inside a laminar soil box.

Objective

The subject of interest is to study the pile behavior from the kinematic effects caused by the soil for the case of a dense crust layer overlying a liquefiable soil layer. Coupled with crust-induced seismic forces, problematic transitions in stiffness can lead to large localized plastic demands in the pile.

Scope

A 1-g shaking table experiment was conducted considering a single reinforced concrete pile embedded in a 3-layer soil system. The model pile of 10 inch diameter was tested in a sloped laminar soil box 69.7” (W) x 154” (L) x 74” (H) to study its response to seismic kinematic loading. Inertial load effects were neglected by designing the specimen without a mass block at the top. The tested specimen was designed at the lower bound of typical design strength (low strength and stiffness). The pile was extended 4D (where D = pile diameter of 10”) above the ground surface and penetrated 7D into a stiff uppermost crust (2.5D thick) overlying a middle saturated loose sand layer (2.5D thick) and a lower dense layer of sand (2.0D thick). Specimen was subjected to varying amplitude ground motions to induce liquefaction and lateral spreading loads. Results indicate significant plastic demands at the crust-liquefiable layer interface.

MODEL DESIGN AND CONSTRUCTION

The laminar soil box is mounted on the uniaxial shake table in the Charles Lee Powell Laboratory at UCSD. The test setup is shown in Fig. 1. The shake table in the south Powell Laboratory has a maximum gravity capacity of 80 kips and a servo controlled dynamic rated actuator with a load capacity of 110 kips. It has a footprint of 10ft x 16ft and a total stroke of 12 inches. The maximum velocity of the shake table is 35 inches per second. The laminar soil box is comprised of 28 stacked frames with rollers sandwiched between the frames. Inside dimensions of the laminar soil box are 69.7” (W) x 154” (L) x 74.0” (H). A single reinforced-concrete pile was placed vertically in the laminar soil box and surrounded by loose saturated #30 silica sand with a target relative density of Dr = 50%. The pile was fixed at the base. The laminar soil box was mounted on concrete blocks to create a gentle slope of approximately 3.5%. The test was conducted at 1-g.

Fig. 1. Laminar soil box on the shake table at UCSD Powell Laboratories.

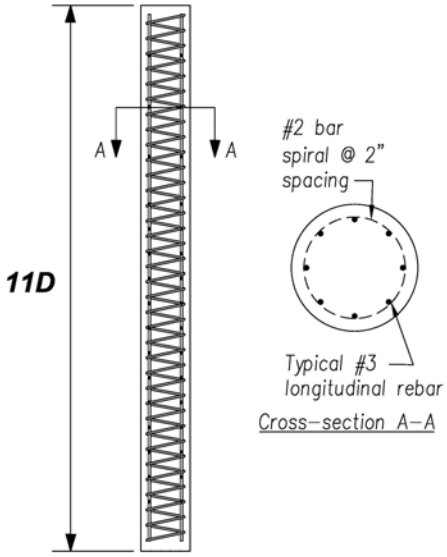

Fig. 2. Construction drawing for reinforced-concrete pile.

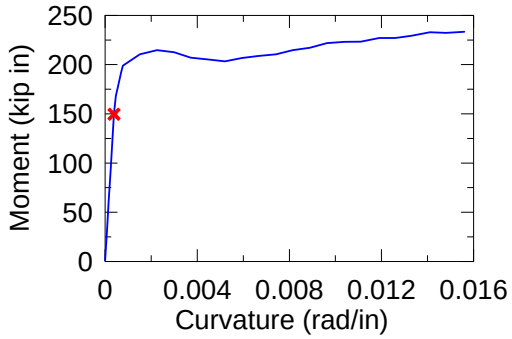

Fig. 3. Moment versus curvature plot for the reinforced-concrete pile circular section. Red "x" denotes values of the yield moment and yield curvature.

Pile

The reinforced-concrete pile was constructed from normal strength concrete, Grade 60 #3 longitudinal reinforcement, and #2 wire spiral for confinement. During casting of the specimen, a concrete slump of 8.5" was measured. From compression tests of 6" diameter cylinders, the day of test concrete strength f'c was 4.52 ksi. Yield strain and strength of the #2 wire spiral and the #3 longitudinal reinforcement are summarized in Table 1 below. The reinforced-concrete pile was 110" long with a diameter of 10". Concrete cover was 1" thick, and the spiral reinforcement spacing was 2" (Fig. 2).

Concrete compression strength and steel reinforcement stress-strain values were used to calculate the moment versus curvature relation for the circular section (Fig. 3). Yield moment of the section was 148 kip in, and yield curvature of the section was 0.00038 rad/in per the analysis by the software program XTRACT.

Table 1. Steel reinforcement stress and strain.

Bar #	Yield Strain and Strength		Ultimate Strain and Strength	
	ε_y	σ_y (ksi)	ε_y	σ_y (ksi)
#2	0.0035	52.4	0.094	62.4
#3	0.0034	65.0	0.150	95.6

Soil Placement

Three layers of soil were placed around the reinforced-concrete pile in the laminar soil box. The bottom-most layer was a dense sand layer, the middle layer was a saturated sand layer, and the topmost layer was a stiff crust layer. Each layer was separated by a plastic sheet, which was intended to mimic an impermeable layer. The same grain size (#30 silica sand) was used for the bottom and middle layers of soil (Fig. 4). The maximum dry density of this sand was 101.0 pcf; the minimum dry density was 80.1 pcf. The minimum void ratio is 0.66; the maximum void ratio is 1.09. Specific gravity is 2.686. (GeoCon report)

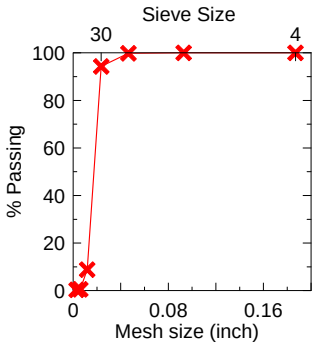

Fig. 4. Grain size distribution test results for #30 silica sand (GeoCon report)

The bottom-most layer of dense sand was placed by dropping moist #30 silica sand from a height of approximately 6 feet to a thickness of approximately 5 inches. This layer was then tamped with a steel plate. Successive layers were built to create a 20 inch thick layer of 2D. Density of the dense sand layer was 99.37 pcf with an initial moisture content of 1.4% and friction angle of 41°. Estimated relative density Dr was 83%. This layer was then overlain with a plastic sheet that was fixed in place.

To achieve a homogeneous saturated soil layer of target relative density Dr = 50% for the middle layer, the method of pluviation was used to place the soil into the laminar soil box. Initial pluviation trials were conducted to determine the best method of placement for the kiln dried #30 silica sand (Fig. 5). A bag of kiln dried sand was suspended over the hopper. This hopper had a series of specifically sized meshes at the beginning and at the end of the tube. Via this tube, the sand was dropped into the container, which contained a certain volume of still water. The sand grains fell from the end of the tube, which was positioned approximately two inches above the water, and fell into the water. The sand grains then subsided gently through the eight inches of water and settled onto the bottom of the container. Sand grains were dropped into the water until a five inch thick lift was achieved. This particular method of placing soil was able to achieve a relatively loose density of soil. The volume of sand that was dropped into the container was measured, and the weight of the bag of sand was measured before and after pluviation. Sand was weighed by a heavy-duty scale with a maximum capacity of 10000 lbs; each tick mark equaled 50 lbs. By using this data, the relative density of the saturated soil layer was estimated. After obtaining a reliable relative density from the pluviation trials, the kiln dried sand was placed into the laminar soil box by using the same method. The saturated sand layer with a thickness of 25" (2.5D) had a density of 117 pcf and a friction angle of 36°. Estimated relative density of the saturated layer was fairly close to the target of 50%.

The topmost 25" thick crust was a 6 sack cement slurry mix. Slurry strength on the day of testing was 746 psi. Density of the crust layer was 132 pcf.

Table 2. Cement slurry mix for crust layer.

Weights per cubic yard	**Yield, cubic feet**
ASTM C-150 Type II/V Cement (lb)	1.15
ASTM C-618 Class F Flyash (lb)	2.65
Concrete Sand (lb)	12.01
Water (lb) (Gal, US)	(63.5) 8.49
Total entrained air (%)	2.70
ASTM C-260 air entrainment (oz)	10.0

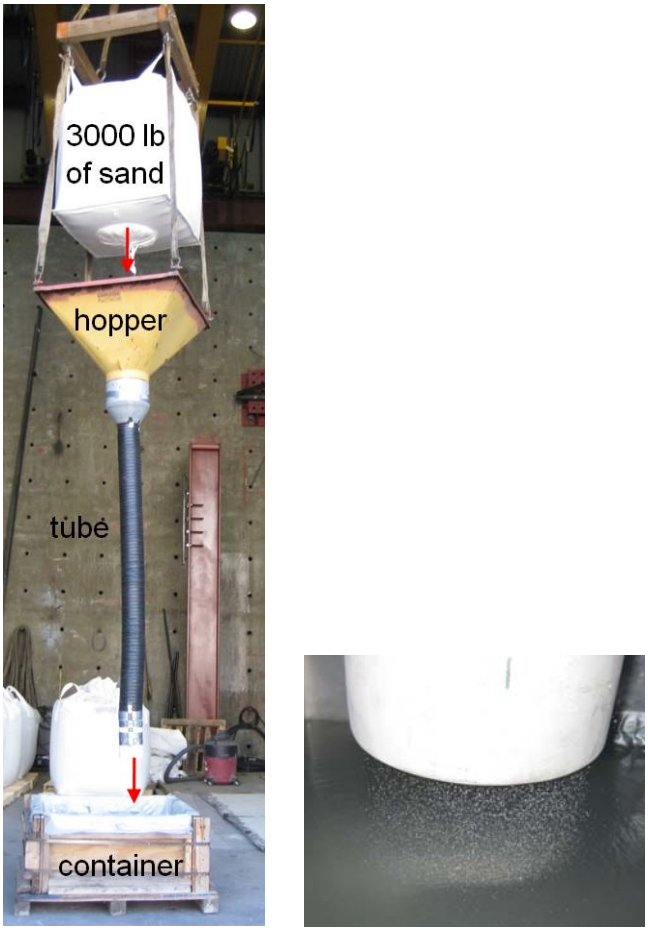

Fig. 5. Pluviation equipment for placing sand at left (hopper and tube with meshes).Trial pluviation container is shown at end of tube. At above right, typical sand falling into standing water.

INSTRUMENTATION

The laminar soil box and the reinforced-concrete pile were instrumented with over one hundred instruments. These instruments included accelerometers, inclinometers, string potentiometers, pore pressure transducers, soil pressure

transducers, and strain gages. Instruments were embedded in the soil layers and in the pile, were attached to the pile, and also attached to the laminar soil box.

In Fig. 6 and Fig. 7, a schematic of the instruments on the laminar soil box and embedded in the soil layers is shown. Accelerometers were placed on the south outside of the laminar soil box. String potentiometers (not shown) were installed to measure the displacement of the south laminar frames. Horizontal accelerometers, pore pressure transducers, and soil pressure transducers were embedded in the soil layers where appropriate along the centerline of the pile within the soil. Instruments at line "A" and "H" are placed 0.5D away from the laminar face of the box liner; instruments at line "B" and "G" are placed 3D away from the respective pile face; instruments at line "C" and "F" are placed 1D from the respective pile face; and instruments at line "D" and line "E" are placed 0.5D from the respective pile face.

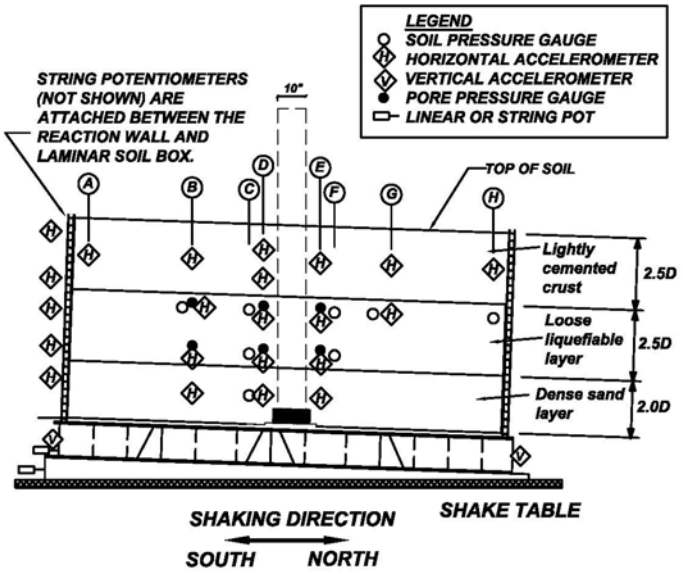

Fig. 6. Schematic (elevation vie)w of instruments used on laminar soil box.

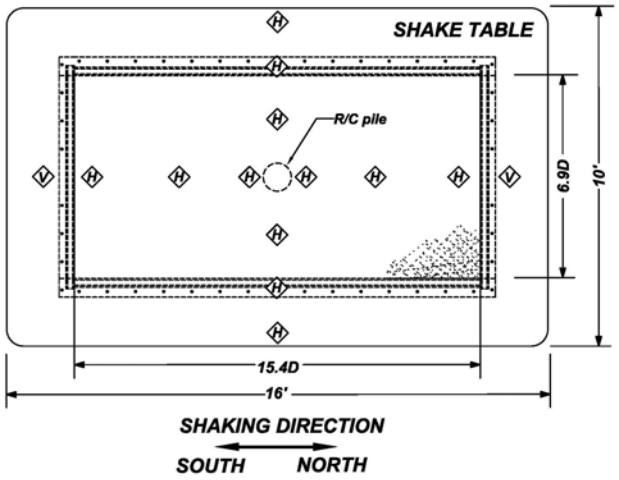

Fig. 7. Schematic (plan view) of instruments used on laminar soil box.

Accelerometers and inclinometers were attached to the surface of the reinforced-concrete pile (Fig. 8). The reinforced-concrete pile was also instrumented with embedded high-elongation strain gages which were placed length-wise (in pairs) on the longitudinal reinforcement (#3 bar) at the extreme south and north locations (Fig. 9).

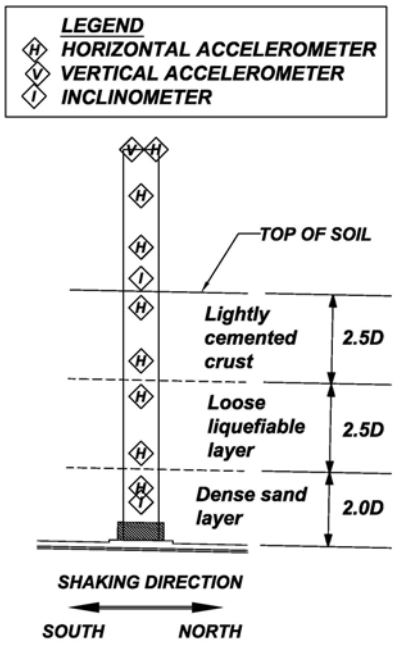

Fig. 8. Schematic of instruments attached to pile.

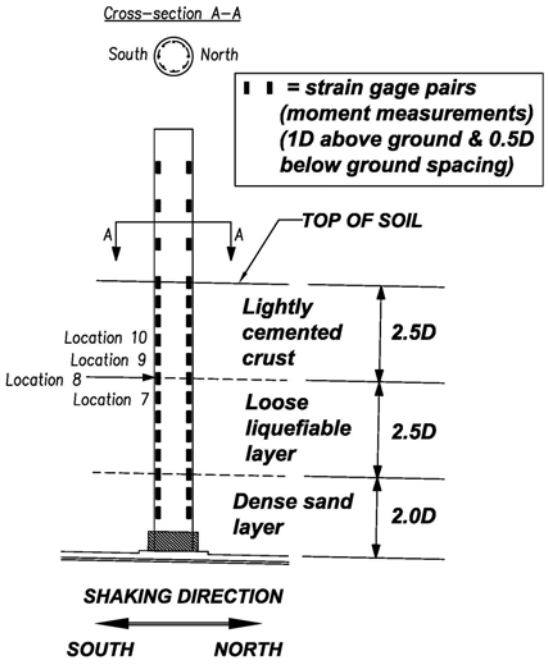

Fig. 9. Schematic of strain gages embedded in reinforced concrete pile.

TEST PROTOCOL

Dynamic base shaking was applied to the specimen. Two scaled earthquake ground motions (Fig. 10) were applied in the course of testing: one from the 1978 Tabas, Iran earthquake (PGA 0.688g) , and the other from the 1995 Kobe, Japan earthquake (PGA 0.356g).

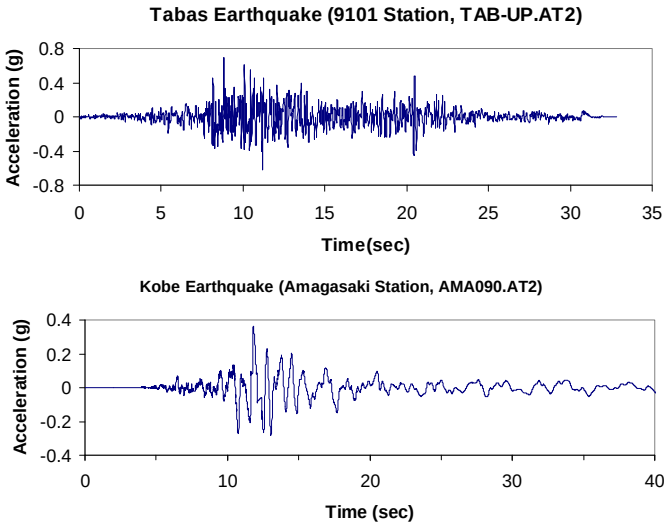

Fig. 10. Time history of ground motions.

From a hammer test to the specimen before applying the ground motions, the first mode frequency of the specimen was measured to be 9.9 Hz with a damping of approximately 1%. This gives the specimen a natural period of approximately 0.63 seconds. Response spectra of the Tabas and the Kobe ground motions show differing maximum response at periods of 0.07 second to 0.2 second and 0.4 second to 1.0 second, respectively.

Testing comprised two days in length. The first day, white noise 1 was applied to the specimen. On the second day, the remaining ground motions in the subsequent table were applied (Table 3). Magnitude of the ground motions were restricted by the limitations of the shake table.

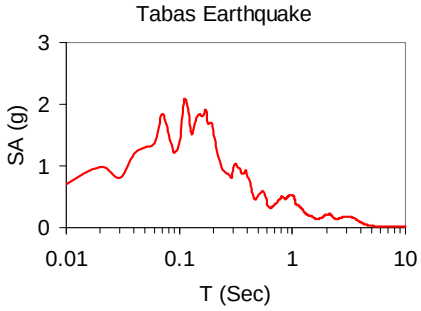

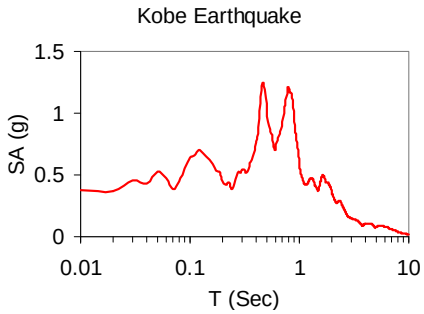

Fig. 11. Response spectra of ground motions.

Table 3. Ground motions applied to specimen.

Ground motion name	Description
White noise 1	0.01g, 0.25 to 50 Hz
White noise 2	0.01g, 0.25 to 50 Hz
Tabas 25%	Scaled by 0.25
Tabas 50%	Scaled by 0.50
Tabas 75%	Scaled by 0.75
Tabas 100%	No scaling
White noise 3	0.01g, 0.25 to 50 Hz
White noise 4	0.01g, 0.25 to 50 Hz
Kobe 75%	Scaled by 0.75
White noise 5	0.01g, 0.25 to 50 Hz

DATA INTERPRETATION/RESULTS

Liquefaction of the saturated soil layer was observed during testing. No cracking or settlement of the crust layer was observed. Due to the strength of the crust layer, no gap between the pile and the crust was visible during inspection between shaking events.

Time history data from the pore pressure instruments are show in Fig. 12 and Fig. 13 for the ground motion inputs of Tabas scaled to 25% and Tabas scaled at 100%. Pore pressure instruments 1, 3, and 5 are closer to the surface of the saturated soil layer, and pore pressure instruments 2 and 4 are near the bottom of the saturated layer. During the Tabas 25% ground motion, liquefaction of the saturated layer is observed from the increasing trend in the pore pressure data. The pore pressure increases and then levels off.

At the later ground motion input of Tabas 100%, a curious trend in the pore pressure data is observed. As the magnitude of the acceleration of the shake table increases, the general trend of the pore pressure data dips in value. When the magnitude of the acceleration decreases, the pore pressure rises. This may be attributed to the phase transformation behavior of the saturated sand layer during strong shaking. The sand is transitioning from contractive to dilatant behavior (and back); these transitions are illustrated by both the sharp decreases in pore pressure and the “dipping” trend of the data.

The pore pressure measurements gradually increase again after time = 22.5 seconds. This coincides with a decrease in the magnitude of the acceleration of the shake table from a negative peak acceleration of 0.45g that tapers gradually to zero. Peak table accelerations from Tabas 100% range from 0.52g to -0.53g. Peak accelerations from Tabas 25% range from 0.16g to -0.14g. Due to the lower magnitude of shaking for Tabas 25%, widespread deliquefaction of the saturated soil layer was not observed.

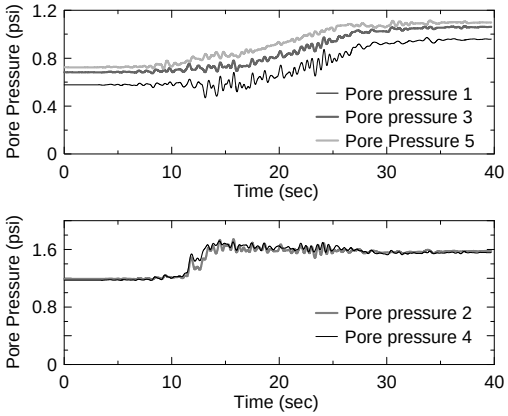

Fig. 12. Pore pressure measurements from Tabas 25% ground motion input.

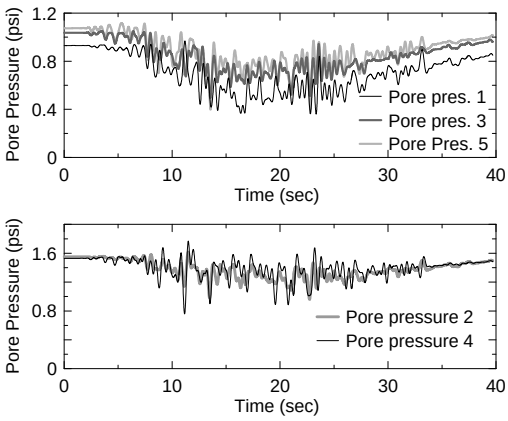

Fig. 13. Pore pressure measurements from Tabas 100% ground motion input.

During testing of the specimen, strain in the longitudinal reinforcement did not reach yield strain until the Tabas ground motion at 100% was applied. At this point in the testing sequence, non-linear strains were observed in the strain gages at location 8 (see previous Fig. 9). Location 8 was just at the interface between the crust and the saturated soil layer. This region with extreme variation in soil stiffness was where the largest strains were expected to be observed (Fig. 14). In the saturated soil layer (location 7), the strains were comparatively much smaller than at the crust to saturated soil interface (location 8). Within the crust region, the accompanying strains were also comparatively lower at strain gage location 9 and 10. The north strain gage at location 9 was no good during the Tabas 100% ground motion, and thus is not shown.

Strains at location 8 showed large changes in the strain that occurred due to the effect of the acceleration of the crust. A small "x" marks this occurrence of large strain for the south side strain gage at time = 11.189 seconds, and a small "o" marks the occurrence for the north side strain gage at time = 13.504 seconds (Fig. 14). These peaks in strain correspond to abrupt accelerations in the crust (Fig. 15). Although there were corresponding peaks in the acceleration records for the shake table and the saturated layer, it was the massive heavy crust layer that had the largest magnitude of acceleration at those particular times, and thus appears to be the main cause of these strains in the pile.

Peak accelerations in the crust are noted with a small "x" for peak negative acceleration and a small "o" for peak positive acceleration. There was a time lag between peak acceleration of the crust and jump in strain for the steel reinforcement. Peak negative acceleration for the crust occurred at time = 11.139 seconds. After 0.05 seconds, the jump in strain for the south strain gage at location 8 occurred. Peak positive acceleration for the crust occurred at time = 13.479 seconds. After 0.025 seconds, the jump in strain for the north strain gage at location 8 occurred.

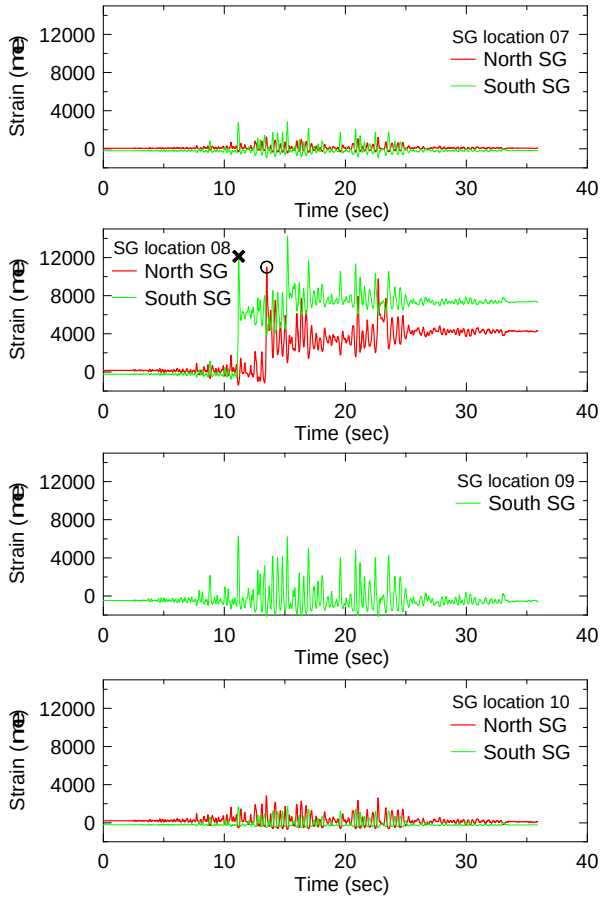

Fig. 14. Embedded pile strain gages time history.

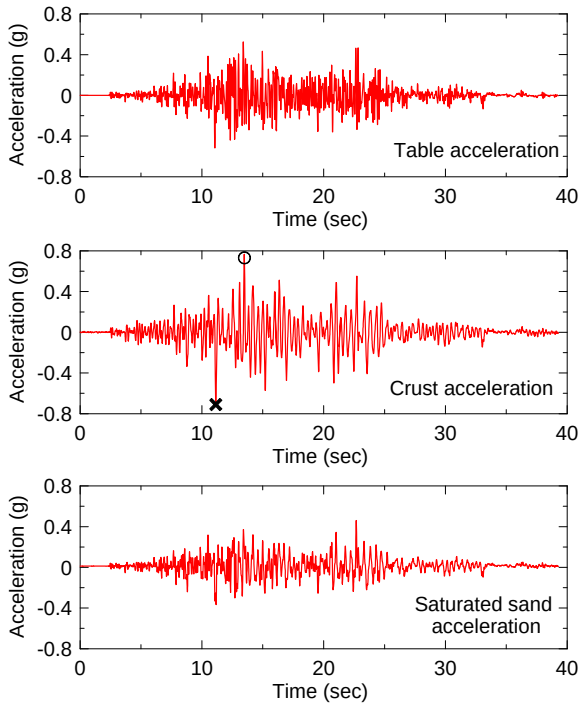

Fig. 15. Recorded accelerations of the shake table, the crust, and the saturated sand layer.

String potentiometers attached to the south side of the laminar soil box show the profile of the laminar frames as the peak negative and positive accelerations of the crust occurred (Fig. 16). Not surprisingly, at peak negative acceleration, the crust was flung southward to a maximum negative displacement of 4.2 inches. The strain gage at location 8 was approximately at the line delineating the boundary between the crust and the saturated sand layer as shown in the profile plots. At peak positive acceleration, the crust displaced towards the north direction a maximum displacement of 5.3 inches. At the end of the ground motion, the shake table returned to its initial displacement, but a profile of the displacement of the laminar frames showed residual displacements which differed for each soil layer.

The saturated sand layer had liquefied and moved down slope northward by 0.41 inches at this time in testing (Tabas 100%), and the crust had similarly displaced northward by 0.23 inches. This amount of movement in the crust was consistent with the movement at the pile top, which was measured to have moved a residual 0.25 inches of displacement. These residual displacements at the top of the pile, for the crust layer, and for the middle and bottom soil layers suggest that the reinforced-concrete pile has deformed from its initial shape during testing.

Physical observations during demolition of the specimen support the recorded strain data. Cracks in the reinforced-concrete pile occurred mainly in the corresponding region of large strains close to the interface between the crust and the saturated soil layer (Fig. 17). On the left photo, the south face of the pile has cracks marked in green ink. Four large cracks were observed for the south face at these elevations on the pile at 59", 49", 47" and 40". These elevations correspond to the general locations 7 to 10. On the right photo, the north face of the pile has cracks marked in red ink. Five cracks are visible on this face at pile elevations of 49", 47", 45" 42" and 37". There elevations again correspond to the region near locations 7 to 10. Some spalling of the cover concrete occurred near location 8. Close ups of the cracked regions show this in more detail (Fig. 18). At location 8, visible cracks extend around the pile (Fig. 19).

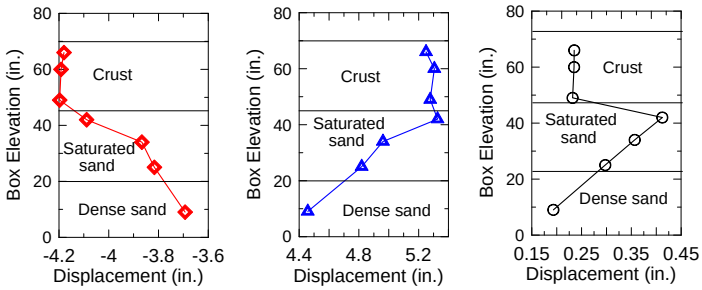

Fig. 16. Horizontal displacement of laminar frames versus vertical height of same frames at time = 11.189 seconds (red, left), time = 13.504 seconds (blue, middle), and at the end (black, right).

Fig. 17. Overall view of south (left) and north (right) faces of the exterior of the pile during demolition (post test).

Fig. 18. Close up of cracked region of pile. South face on left; north face on right.

Fig. 19. Cracked pile at location 8 (at the interface between crust and saturated sand layer).

Non-linear behavior of the reinforced-concrete pile was observed in the moment and curvature behavior of the section. From Fig. 20, the calculated curvature time history of the same region for the pile shows maximum curvature at the boundary between the stiff crust layer and the saturated soil layer. Similar trends are observed for the moment (Fig. 21). These moments are derived from a simple "look up" function that is based on the sectional moment-curvature plot from the software program XTRACT.

The value of the curvature and moment along the length of the pile at certain times during ground motion Tabas 100% is shown in Fig. 22. Again, these profile correspond to the moments in time of peak negative acceleration and peak positive acceleration of the crust. From the curvature profiles, a slight double curvature of the pile is observed. This double curvature does not appear to occur when the pile is at rest. A permanent kink appears to have been formed at crust to saturated soil boundary instead.

Additionally, opposite signs for the value of the moments were generated at the bottom of the pile and at the interface region. For the leftmost moment profile in Fig. 22, the moment at the bottom of the pile in positive and the moment at the interface region is negative. Similarly, the middle moment profile plot shows a large negative moment at the bottom of the pile and positive moment at the boundary interface.

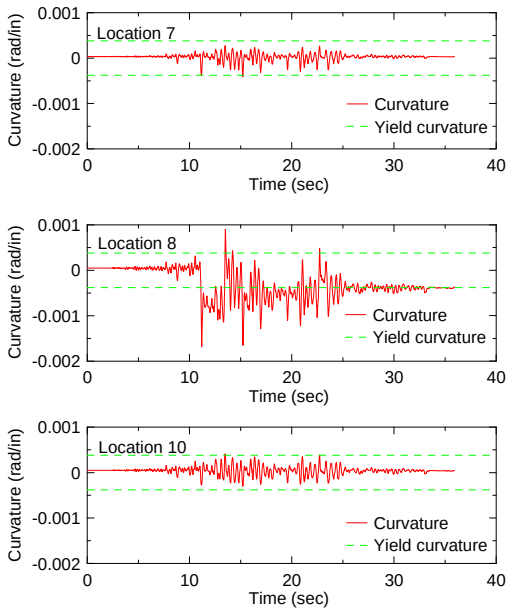

Fig. 20. Curvature time history for selection locations (Tabas 100%).

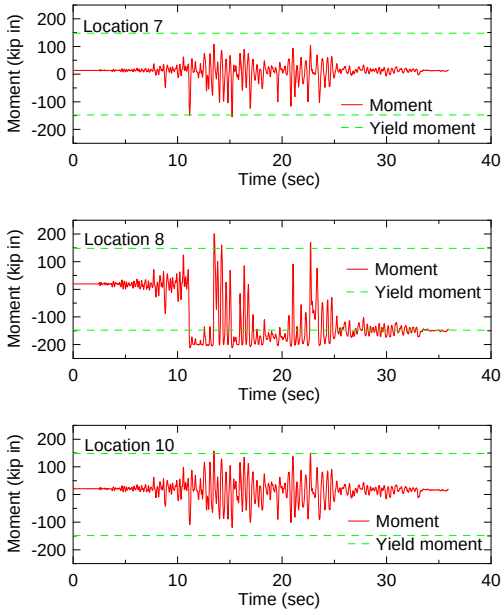

Fig. 21. Moment time history for selected locations (Tabas 100%).

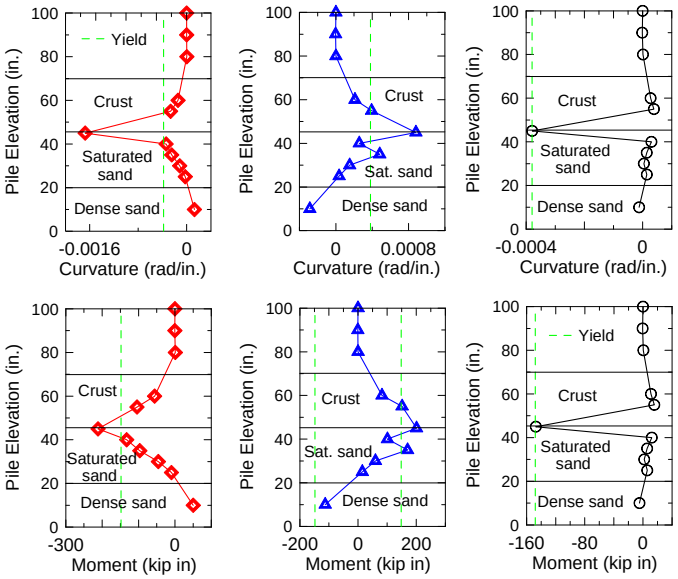

Fig. 22. Curvature and moment profiles versus the pile length at time = 11.189 seconds (red, left), time = 13.504 seconds (blue, middle), and at the end (black, right).

CONCLUSIONS

A 1-g shaking table experiment was conducted considering a single reinforced concrete pile embedded in a 3-layer soil system. The pile was tested in a sloped laminar soil box, in an effort to investigate its response to seismic kinematic loading. Inertial load effects were minimized by designing the specimen without a mass block at the top of the pile. The three-layer soil system was a stiff uppermost crust (2.5D thick) overlying a middle saturated loose sand layer (2.5D thick) and a bottommost dense layer of sand (2.0D thick). The specimen was subjected to varying amplitude ground motions to induce liquefaction and lateral spreading loads.

Liquefaction and downward sliding of the crust was was observed. Although the reinforced-concrete pile behaved linearly for a portion of the test series, at larger magnitude shakes plastic behavior of the pile was observed. At the interface between the stiff crust and the soft saturated soil layer, non-linear strains, and thus plastic behavior of the pile, were measured, and post-yield curvature and moments were reliably calculated. Physical observations during post-test excavation confirmed the observed nonlinear behavior. The experimental dataset will provide useful for evaluation of design methods and modeling tools for considering kinematic seismic loading on piles.

ACKNOWLEDGMENTS

The research support by the National Science Foundation (NSF) under the CAREER program, grant number CMMI-0729483 is gratefully acknowledged. Any opinions, findings, and conclusions expressed are those of the authors, and do not necessarily reflect those of the sponsoring organization. Special thanks to the staff at the University of California, San Diego Powell laboratories, and in particular Dr. Chris Lathman, Mr. Andy Gunthardt and Mr. Paul Greco.

REFERENCES

Abdoun, T. and Dobry, R. [2002]. "Evaluation of pile foundation response to lateral spreading", Soil Dynamics and Earthquake Engineering, No. 22, pp. 1051-1058.

Abdoun, T., Dobry R., O'Rourke, T., and Goh, S.H. [2003]. "Pile Response to Lateral Spreads: Centrifuge Modeling", Journal of Geotechnical and Geoenvironmental Engineering, Vol, 129, No. 10, pp. 869-878.

Ashford, S.A., and Jakrapiyanun, W. [2001]. "Design and Verification of the UCSD Laminar Container." Structural Systems Research Project Report No. TR-2001/07, Department of Structural Engineering, University of California, San Diego.

Brandenberg, S.J., Boulanger, R.W., Kutter, B.L, and Chang, D. [2005] "Behavior of Pile Foundations in Laterally Spreading Ground during Centrifuge Tests," Journal of Geotechnical and Geoenvironmental Engineering, Vol. 131, No. 11, pp. 1378-1391.

Das, B. [2004]. Foundation Engineering, 5th edition, Brooks/Cole-Thomson Learning Inc., Pacific Grove, California.

Dobry, R., Abdoun, T., O'Rourke, T, and Goh, S.H. [2003]. "Single Piles in Lateral Spreads: Field Bending Moment Evaluation", Journal of Geotechnical and Geoenvironmental Engineering, Vol, 129, No. 10, pp. 879-889.

GeoCon Incorporated, Soils Report on the #30 silica sand.

Martin, G.R. and Chen, C.Y. [2005]. "Response of piles due to lateral slope movement." Computers and Structures, Vol 83, pp. 588-598.

Tokimatsu, K. and Asaka, Y. [1998]. "Effects of Liquefaction-Induced Ground Displacements on Pile Performance in the 1995 Hyogoken-Nambu Earthquake", Soils and Foundations, Special Issue, pp. 163-177.

Tokimatsu, K., Suzuki, H., and Sato, M. [2005]. "Effects of inertial and kinematic interaction on seismic behavior of pile with embedded foundation", Soil Dynamics and Earthquake Engineering, No. 25, pp. 753-762.

Wilson, D.W., Boulanger, R.W., and Kutter, B.L. [2000]. "Observed Seismic Lateral Resistance of Liquefying Sand", Journal of Geotechnical and Geoenvironmental Engineering, Vol. 126, No. 10, pp. 898-906.

Yasuda, S. and Berrill, J.B. [2000]. "Observations of the Earthquake Response of Foundations in Soil Profiles Containing Saturated Sands", *1st International Conference on Geotechnical and Geological Engineering.* Melbourne, Australia, Issue Lecture, pp. 1441-1471.